MNRAS **435,** 242–254 (2013)
Advance Access publication 2013 August 8
doi:10.1093/mnras/stt1289

Bayesian asteroseismology of 23 solar-like *Kepler* targets

M. Gruberbauer,[1]⋆ D. B. Guenther,[1] K. MacLeod[1] and T. Kallinger[2]

[1]*Institute for Computational Astrophysics, Department of Astronomy and Physics, Saint Mary's University, Halifax, NS B3H 3C3, Canada*
[2]*Institute for Astrophysics, University of Vienna, Türkenschanzstrasse 17, A-1180 Vienna, Austria*

Accepted 2013 July 12. Received 2013 July 11; in original form 2013 June 4

ABSTRACT

We study 23 previously published *Kepler* targets to perform a consistent grid-based Bayesian asteroseismic analysis and compare our results to those obtained via the Asteroseismic Modelling Portal. We find differences in the derived stellar parameters of many targets and their uncertainties. While some of these differences can be attributed to systematic effects between stellar evolutionary models, we show that the different methodologies deliver incompatible uncertainties for some parameters. Using non-adiabatic models and our capability to measure surface effects, we also investigate the dependency of these surface effects on the stellar parameters. Our results suggest a dependence of the magnitude of the surface effect on the mixing length parameter which also, but only minimally, affects the determination of stellar parameters. While some stars in our sample show no surface effect at all, the most significant surface effects are found for stars that are close to the Sun's position in the Hertzsprung–Russell diagram.

Key words: methods: statistical – stars: oscillations.

1 INTRODUCTION

Ultraprecise long-term photometric time series from space have revolutionized the study of stellar variability in recent years. The *Convection, Rotation and Planetary Transits* (*CoRoT*; Michel et al. 2008) and the *Kepler* (Borucki et al. 2010) space telescopes in particular have produced high-quality data sets for thousands of stars in order to detect planets down to Earth size and below. Particularly interesting for the study of stellar interiors and stellar evolution is their ability to detect solar-type oscillations from giants to subdwarfs. The pulsational characteristics of these stars adhere, at least to a very good first approximation, to scaling relations (e.g. Huber et al. 2011) permitting the study of large populations of stars with 'ensemble asteroseismology' (Chaplin et al. 2011) and even Galactic archaeology (Miglio et al. 2013).

The same information can also be exploited to infer the parameters of individual stars, e.g. to better constrain their planets' properties. For stellar astrophysics, however, the ultimate goal is to use asteroseismology to study stellar interiors. Instead of direct inversion of the pulsation information, asteroseismology usually employs a comparison between observed and modelled pulsation frequencies (e.g. Guenther & Brown 2004). Various new tools have been developed to facilitate a state-of-the-art version of such a comparison using different approaches, such as the Asteroseismic Modelling Portal (AMP; Metcalfe, Creevey & Christensen-Dalsgaard 2009) and Bayesian grid-based analysis (Gruberbauer, Guenther & Kallinger 2012, hereafter Paper I). The major differences between these methods lie in their different statistical basis and their different applications of what is known as the surface effect correction (see Paper I for an in-depth discussion). Already, the AMP has been used to analyse some *Kepler* targets in detail and to compare the results with those from other modellers (Metcalfe et al. 2010, 2012). Such a comparison is advantageous, because asteroseismic modelling often relies on a specific set of stellar models with a specific set of input physics. Slight systematic differences among these models are therefore not only plausible but unavoidable, resulting in underestimated uncertainties. A different approach is to study a larger sample of stars self-consistently with one particular method and model base to facilitate a pool of results to be compared with other researcher's results (Mathur et al. 2012).

In this paper we re-examine some of the previously published studies based on *Kepler* data with a strong emphasis on AMP results, employing our own set of models and our Bayesian method described in Paper I. We will discuss how the results differ and whether the methodologies themselves introduce systematic deviations. We will also perform the first detailed study on surface effects for a sample of stars with our flexible method.

2 METHODS, MODELS AND OBSERVATIONS

2.1 Target selection and observations

In order to investigate the impact of the stellar models and methodologies in the most general sense, we analyse stars for which the p-mode frequency sets and detailed prior information used in previous

⋆E-mail: mgruberbauer@ap.smu.ca

asteroseismic fitting procedures are available in the literature. We furthermore constrain ourselves to stars that do not show strong signatures of deviations from the asymptotic relation, i.e. avoided crossings such as in KIC 11026764 (Metcalfe et al. 2010). While those signatures are very valuable for asteroseismic inferences and can be easily taken into account with our method as mentioned in Paper I, they would constitute special cases in the comparison between methods. We therefore postpone such an analysis to a future paper and restricted ourselves to 20 of the 22 stars analysed by Mathur et al. (2012, hereafter Mathur20), the solar analogues 16 Cyg A&B (Metcalfe et al. 2012), and the planet-host Kepler-36 (Carter et al. 2012). Where available in the previously cited papers, we use prior constraints on $\log T_{\rm eff}$, $\log L/\mathrm{L}_\odot$, Z/X (adopting $[\mathrm{Fe/H}]_\odot = 0.0245$) and $\log g$. Following our description in Paper I, these prior constraints are modelled as separate Gaussian probability distributions.

As is common in recent asteroseismic analyses, we treat the frequency of maximum power $\nu_{\rm max}$ as an additional and independent observable by using the scaling relation

$$\nu_{\rm max,mod} \approx \frac{M/\mathrm{M}_\odot \left(T_{\rm eff}/\mathrm{T}_{\rm eff,\odot}\right)^{3.5}}{L/\mathrm{L}_\odot} \nu_{\rm max,\odot}, \quad (1)$$

where we employ the solar value $\nu_{\rm max,\odot} = 3120.0 \pm 5\,\mu$Hz given by Kallinger et al. (2010) based on VIRGO data. For Mathur20, the observed values and uncertainties of $\nu_{\rm max}$ have been taken from Mathur20, and for Kepler-36 we have used the value published in Carter et al. (2012). For 16 Cyg A&B, we have determined the values ourselves by performing a Bayesian multicomponent model fit, consisting of a flat background, three super-Lorentzian profiles and a Gaussian power hump, to the power density spectra of both data sets.[1] In this case, the central frequency of the Gaussian power hump and the corresponding uncertainties are interpreted as a good proxy for $\nu_{\rm max}$. The method employs the nested sampling algorithm MULTINEST (Feroz, Hobson & Bridges 2009) and is described in more detail in Kallinger et al. (2010). We find $\nu_{\rm max} = 2215.6 \pm 6.5\,\mu$Hz for 16 Cyg A, and $\nu_{\rm max} = 2571.9 \pm 12.6\,\mu$Hz for 16 Cyg B.

2.2 Models

A wide parameter range has to be spanned in order to perform a meaningful grid-based analysis. We therefore employed YREC (Demarque et al. 2008) to produce a set of dense grids covering a wide range in initial masses, and several values for the initial helium mass fraction Y_0, initial metal mass fraction Z_0 and mixing length parameter $\alpha_{\rm ml}$.

Our model tracks begin as completely convective Lane–Emden spheres (Lane 1869; Chandrasekhar 1957) with the stellar age reset to zero when the star crosses the birthline ($10^{-5}\,\mathrm{M}_\odot\,\mathrm{yr}^{-1}$; Palla & Stahler 1999). They are evolved from the Hayashi track (Hayashi 1961) through the zero-age-main-sequence (ZAMS) to the base of the red giant branch. Constitutive physics include the OPAL98 (Iglesias & Rogers 1996) and Alexander & Ferguson (1994) opacity tables, as well as the Lawrence Livermore equation of state tables (Rogers 1986; Rogers, Swenson & Iglesias 1996). Convective energy transport was modelled using the Böhm-Vitense mixing length theory (MLT; Böhm-Vitense 1958). The atmosphere is implemented using Eddington grey atmosphere. Nuclear reaction cross-sections were taken from Bahcall, Pinsonneault & Basu (2001) and the nuclear reaction rates from table 21 in Bahcall & Ulrich (1988). The effects of helium and heavy element diffusion (Bahcall, Pinsonneault & Wasserburg 1995) were included. The model grid contains models with $M/\mathrm{M}_\odot$ from 0.8 to 1.3 in steps of 0.01 and Y_0 from 0.210 to 0.315 in steps of 0.005. Furthermore, Z_0 is varied from 0.005 to 0.04 in steps of 0.005, but with the overall constraint that $X_0 \geq 0.68$. Lastly, we also vary $\alpha_{\rm ml}$ from 1.8 to 2.4 in steps of 0.1.

The pulsation spectra were computed using the stellar pulsation code of Guenther (1994), which solves the linearized, non-radial, non-adiabatic pulsation equations using the Henyey relaxation method. The non-adiabatic solutions include radiative energy gains and losses but do not include the effects of convection. We estimate the random 1σ uncertainties of our model frequencies to be of the order of 0.1 μHz. These uncertainties are properly propagated into all further calculations.

2.3 Bayesian asteroseismic grid fitting

Our Bayesian fitting method is explained in detail in Paper I, and it has been previously applied to analyse the Sun (Gruberbauer & Guenther 2013). We compare theoretical ($f_{\rm m}$) and observed ($f_{\rm o}$) frequencies by calculating the likelihood that the two values agree were it not for the presence of random and systematic errors, i.e.

$$f_{\rm o} - f_{\rm m} = \gamma\Delta + e. \quad (2)$$

Here, the random errors e are assumed to be independent and Gaussian. The systematic errors $\gamma\Delta$ in the case of solar-like stars are assumed to be similar to 'surface effects'. At higher orders, observed frequencies are systematically lower than model frequencies, and the absolute frequency differences increase with frequency. This is modelled by introducing Δ as free parameters for each observed mode and by setting $\gamma = -1$.

These Δ terms are then allowed to become larger at higher radial orders. The upper limit $\Delta_{\rm max}$ for each model frequency $f_{\rm m}$ is determined by the large frequency separation and a power law similar to the standard correction introduced by Kjeldsen, Bedding & Christensen-Dalsgaard (2008) so that

$$\Delta_{\rm max} = \Delta\nu \left(\frac{f_{\rm m}}{f_{\rm max,m}}\right)^b, \quad (3)$$

where $b = 4.9$, $\Delta\nu$ is the large frequency separation of the corresponding model and $f_{\rm max,\,m}$ is the frequency of the highest order in the model.[2]

The Δ parameter is incorporated in a completely Bayesian fashion, using a β prior to prefer smaller values over larger ones (see Paper I for more details). In addition, we always allow for the possibility that a mode is not significantly affected by any kind of systematic error by explicitly including the null hypothesis, that is by combining the probabilities of two hypotheses: one with and one without the Δ parameter. Altogether, this allows us to fully propagate uncertainties originating from the surface effects, or other potential systematic differences, into all our results. At the same time it gives us more flexibility than the standard surface-effect correction. Whereas the latter prescribes a fixed power-law behaviour for the actual surface effects, our method only prescribes such a behaviour

[1] Note that only Q7 data obtained between 2010 September to 2010 December have been used in Metcalfe et al. (2012). We therefore restrict ourselves to this data set as well.

[2] This means that for the highest order in the model $\Delta_{\rm max} = \Delta\nu$ and guarantees that we do not introduce ambiguities in the radial orders by implementing the Δ terms.

for the *upper limits* of the surface effects for the individual radial model frequencies.

For each model in our grid, all the likelihood terms from the different frequencies are combined to yield an overall weighted likelihood for the model, where the weights are provided either via prior information or using ignorance priors (i.e. information that simply encodes the dimension of the grid). These weights provide correctly normalized probabilities that allow us to derive distributions for all model properties (e.g. mass, age, fractional radius of the base of the convection zone $R_{\rm BCZ}$, mixing length parameter $\alpha_{\rm ML}$ and so on).

In summary, we obtain probabilities for every evolutionary track in our grid, and within the tracks also for every model. We also obtain the correctly propagated distributions for systematic errors so that the model-dependent surface effect can be measured. In order to fully resolve the changes in stellar parameters and details in the stellar-model mode spectra, we oversample the evolutionary tracks via linear interpolation until the (normalized) probabilities no longer change significantly. Eventually, we obtain so-called evidence values, equivalent to the prior-weighted average likelihood, for the grid as a whole. These could, in principle, be used to perform a quantitative evaluation of different input physics (see Gruberbauer & Guenther 2013) or even different stellar evolution and pulsation codes. We will use them in this study to analyse the significance of the measured surface effects.

In order to facilitate this, we propose two alternative systematic error models in addition to the standard surface effect (SSE) model described above. First, we employ a less restrictive systematic error model where

$$\Delta_{\rm max} = \Delta\nu/2 \tag{4}$$

for every frequency of each particular model. Furthermore, the observed frequencies are allowed to deviate in either direction (first $\gamma = 1$ is evaluated, then $\gamma = -1$ follows and then both results are combined using the sum rule). We call this model the 'arbitrary systematic error' (ASE) model since it allows, in principle, very large differences between observed and calculated frequencies without prescribing any systematic behaviour or preferred sign. Note that this is not equivalent to simply increasing the Gaussian uncertainties of the observed frequencies to $\Delta\nu/2$.

Finally, we will also employ a third error model which only consists of the probabilities obtained without any Δ parameters. This model therefore assumes that no systematic errors are present so that $f_{\rm o} - f_{\rm m} = e$. We will call this the 'no systematic error' (NSE) model. Together, the three systematic error models will allow us to estimate the significance of surface effects or other systematic differences between observed and calculated frequencies.

3 DEPENDENCE OF SURFACE EFFECTS ON NON-ADIABATICITY AND MIXING LENGTH

The advantage of our method to include systematic frequency errors over the standard surface correction is its universality. The SSE exponent of $b = 4.9$ as obtained by Kjeldsen et al. (2008) has been derived for adiabatic pulsation frequencies and for a solar-calibrated model with a calibrated parametrization of the mixing length.[3] More advanced pulsation models and different stellar models (see e.g. Grigahcène et al. 2012) are not necessarily consistent with such a relation. This is also the case for our non-adiabatic pulsation frequencies. Since the only way to improve our modelling of outer layers is to compare more advanced models to observations, it is necessary to relax the constraint of a definite empirical surface correction relation dependent on adiabatic pulsation codes. Aside from the surface effect, our method also allows various other kind of parametrization for systematic errors, such as our ASE model.

The drawback of our method, as discussed in Paper I, is that in the absence of strong prior information about the stellar parameters, a lack of lower order modes will potentially result in an underestimated magnitude of the surface effects. This follows from the fact that we always obtain the most probable result given our state of information including the new data set; if we cannot constrain the stellar model parameters using our prior knowledge, the pulsation frequencies are our only reference. When conditions are encountered under which the empirical correction law of Kjeldsen et al. (2008) does not apply, or if one rejects such a correction on other grounds, we have to evaluate the models acknowledging the presence of less well-specified systematic errors.

As described in Paper I, neglecting lower order modes leads to overestimated $\alpha_{\rm ml}$, mass and metallicity for the Sun, simply because such models can fit the higher order modes better. The same models cannot fit the lower order modes as well, but when they are not included in the list of fitted modes no penalty ensues. For stars other than the Sun, we usually do not have a complete list of lower order modes, nor do we have as accurate non-seismic constraints (e.g. mass, luminosity, age). Even in such cases, however, stellar metallicity, $T_{\rm eff}$ and L can be estimated from spectroscopic and photometric observations. Furthermore, equation (1) reveals that $\nu_{\rm max}$ provides valuable if approximate constraints for the fundamental parameters, including the stellar mass, in particular when spectroscopic constraints are available.

Two adjustable parameters of the stellar model, the helium abundance and $\alpha_{\rm ml}$, affect the structure of the surface layers. The mixing length parameter is normally tuned to produce a model of the Sun at the observed composition and (meteoritic) age that matches the limb-darkening-corrected radius of the Sun. The helium abundance is either derived also from a tuned model of the Sun, matching its luminosity, or extrapolated from the observed rate of Galactic nucleosynthesis. Both the helium abundance and the $\alpha_{\rm ml}$ affect the depth of the convection zone (i.e. the fitted adiabat) and the temperature gradient in the superadiabatic layer (SAL)[4] via the MLT. We stress that the mixing length parameter of the MLT is used primarily to control the efficiency of convection and its adjustment is primarily used to fix the radius of the star. As is well known for the case of the Sun the MLT does not correctly predict the temperature gradients in the SAL so even though it may be providing an accurate radius for the star it may, at the same time, be providing a poor model of the SAL (e.g. Robinson et al. 2003). The surface effect is sensitive to $\alpha_{\rm ml}$ since the p-mode frequencies are sensitive to the SAL. But at the same time the large frequency spacings are also sensitive to the $\alpha_{\rm ml}$ via its effect on the star's radius. The interplay of the two effects of the mixing length parameter on the frequencies makes it difficult to isolate the surface effect completely from $\alpha_{\rm ml}$.

Fig. 1 shows the effect of fitting one of the stars in our sample, KIC 8006161, to a specific evolutionary track with $M = 1.11\,{\rm M}_{\odot}$, $Y_0 = 0.22$ and $Z_0 = 0.04$, but varying values of $\alpha_{\rm ml}$ (note that

[3] As explained in the previous section, technically we also use $b = 4.9$ for our surface effect modelling, but the exponent is only employed to derive an upper limit for the surface effect for each mode. This does not enforce the usual power-law-like behaviour of the surface effect.

[4] Below the SAL, the temperature gradient is adiabatic.

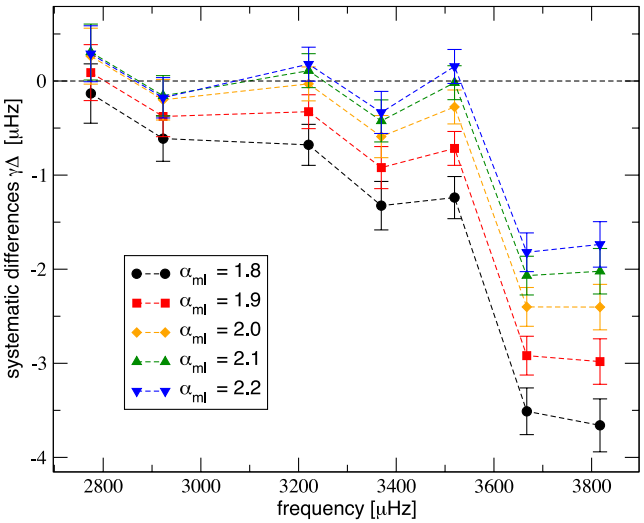

Figure 1. Systematic differences between observed and computed $l = 0$ modes for KIC 8006161 when fitted by models with varying mixing length but otherwise fixed initial parameters.

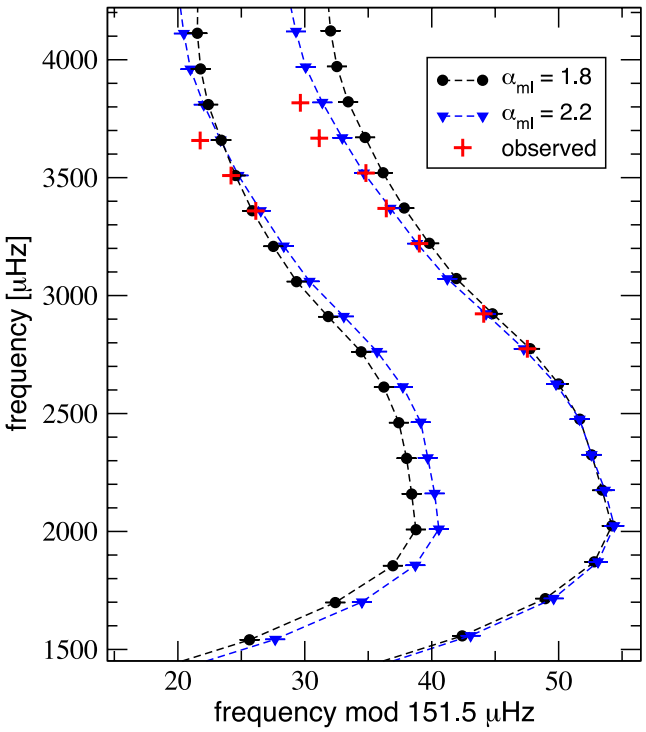

Figure 2. Echelle diagrams for the $l = 0$ (right-hand sequence) and 2 (left-hand sequence) modes of KIC 8006161 and two models with different $\alpha_{\rm ml}$. The uncertainties of the observed frequencies are of the order of the symbol size.

these models are not equivalent to our most probable models as determined in the next section). At the highest frequencies, the larger $\alpha_{\rm ml}$ values clearly reduce the measured surface effect by almost 50 per cent, and the effect is even more pronounced at the lower orders.[5] On the other hand, the plot suggests that at the lowest observed radial order, the frequencies for the higher $\alpha_{\rm ml}$ models are somewhat too low. Fig. 2 presents the echelle diagram for the $l = 0$, 2 modes of the $\alpha_{\rm ml} = 1.8$ and 2.2 models. We observe that if the set of $l = 2$ modes extended below ∼3000 μHz, we would be able to clearly distinguish between these two models. At the $l = 0$ orders below ∼2000 μHz the two models show small but systematic differences as well. With the current set of observed modes, however, we cannot clearly determine whether a lower or higher mixing length parameter value is more probable. Yet, we want to find the model with the smallest surface effects that still fits all other constraints. Therefore, in our example the higher $\alpha_{\rm ml}$ values become more probable automatically. As long as we have limited knowledge on the magnitude of the surface effects across the Hertzsprung–Russell (HR) diagram, however, this increase in probability might not be warranted. In the given example, it does seem as if the $\alpha_{\rm ml} = 2.2$ model is more consistent with the observed small spacing, but we know that the solar-calibrated value is closer to $\alpha_{\rm ml} \sim 1.8$, so deviations from this value should not be taken lightly.[6] Nonetheless, studying the possible variation of the mixing length parameter across the HR diagram and its interplay with the surface effects is important, so setting a fixed (calibrated) value is also not desirable.

We therefore propose the following solution: we perform our analysis using three different approaches to constraining the mixing length. The first approach is to not use any prior on $\alpha_{\rm ml}$. The second approach is to employ a Gaussian prior with $\alpha_{\rm ml} = 1.8 \pm 0.075$, based on the solar calibrated value. The standard deviation of the prior (0.075) is somewhat arbitrary, but we choose it to permit deviations from the calibrated value in the presence of strong evidence. As the maximum value of $\alpha_{\rm ml}$ in our grid is 2.4, such a model would represent an a priori 8σ outlier. For such a model to still be more probable, it would require differences in likelihood of about 14 orders of magnitude, and therefore a large amount of evidence from the frequencies and the fit to the other stellar parameters. The prior should therefore only lead to $\alpha_{\rm ml} > 2.1$ for stars that can be matched very well both in terms of their frequencies and in terms of their fundamental parameters. Lastly, the third approach is to constrain ourselves to $\alpha_{\rm ml} = 1.8$ in reference to the Sun-calibrated value for Eddington atmospheres. This set of different constraints on $\alpha_{\rm ml}$ will allow us to show its impact on the stellar parameters and the surface effects. By comparing the Bayesian evidence for the result obtained with different priors, we can also quantify the formal preference of one prior over the others.

As an example, we present the results for the surface effect analysis of KIC 8006161, based on the complete grid rather than just one evolutionary track, in Fig. 3. While for this star the prior does not have a big effect at the lower order modes, we obtain significantly larger surface effects beyond 3300 μHz with the $\alpha_{\rm ml}$ priors. Even with the Gaussian $\alpha_{\rm ml}$ prior, as will be shown below, the most probable posterior value for $\alpha_{\rm ml}$ lies above 1.8.

4 RESULTS

As described in the previous sections, we have analysed all 23 stars in our sample with the same grid, using priors on their fundamental parameters if available and three different models relating to the

[5] It is necessary to point out, however, that for adiabatic frequencies, the relative impact of the mixing length is not as big as for the non-adiabatic frequencies.

[6] Note that such deviations are also a non-negligible problem when applying the standard surface correction since it relies on the solar-calibrated values at the solar mixing length parameter.

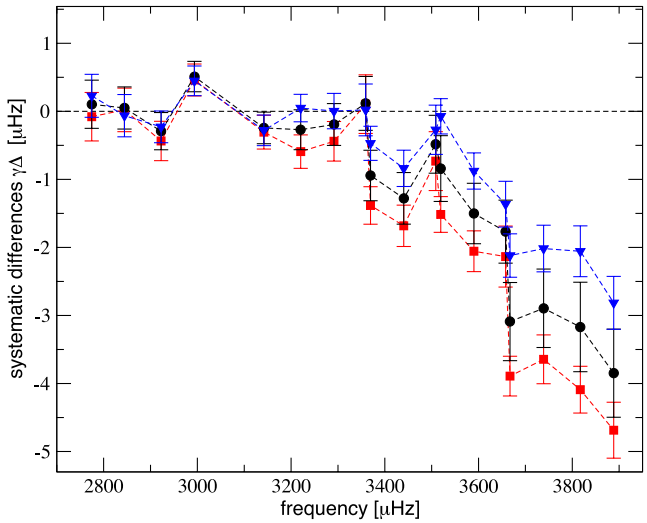

Figure 3. Systematic differences between all observed and computed modes of KIC 8006161 for the whole grid, calculated with (black circles) and without (blue triangles) $\alpha_{\rm ml}$ prior. Results for only the $\alpha_{\rm ml} = 1.8$ models (red squares) are also shown.

treatment of systematic errors. Moreover, we perform this analysis three times, first setting $\alpha_{\rm ml} = 1.8$, then with a Gaussian prior and lastly without a prior on $\alpha_{\rm ml}$. The results are given in Table 1, and the most probable $\alpha_{\rm ml}$ priors and surface effect models are also indicated.

4.1 The influence of the $\alpha_{\rm ml}$ priors

Before we move on to a comparison to the literature, we first study the effect of the $\alpha_{\rm ml}$ priors on our results. Fig. 4 shows the posterior mean values and uncertainties of $\alpha_{\rm ml}$, M, Y_0, $\log g$, Z/X and age for all stars and compares the results with and without the Gaussian $\alpha_{\rm ml}$ prior. The Gaussian $\alpha_{\rm ml}$ prior leads to slightly lower values of $\alpha_{\rm ml}$ as was expected from the discussion in Section 3. Furthermore, the stellar masses are also slightly lower with an average difference $\langle \Delta M \rangle = -0.021\,{\rm M}_\odot$, and, although there is a larger scatter in Y_0, slightly larger values in the initial helium mass fraction are also preferred with an average difference of $\langle \Delta Y_0 \rangle = 0.008$. On the other hand, $\log g$ remains basically unaffected as expected, since the radius of the stars are well constrained by the large spacings (as we will see below, this also extends to a comparison with the other $\alpha_{\rm ml}$ prior and the literature). Z/X and age also do not show strong systematic effects. Nonetheless, the latter does exhibit a strong outlier with 16 Cyg B, for which the age changes from 9.279 ± 0.473 to 6.532 ± 0.281 Gyr. Note that even though the Bayesian evidence is clearly in favour of the older model, the younger value is much more reasonable, given the results from Metcalfe et al. (2012) and also given the value of the age for 16 Cyg A. This is a good test case for the impact of the $\alpha_{\rm ml}$ prior.

A comparison of the results from the Gaussian prior and the fixed $\alpha_{\rm ml} = 1.8$ prior is presented in Fig. 5. In general, the results fall in line with our expectations: the mass is now slightly larger for the Gaussian prior with $\langle \Delta M \rangle = 0.014$, and Y_0 is slightly smaller with $\langle \Delta Y_0 \rangle = -0.005$. Z/X and age values are again quite comparable except for a few outliers. In general the systematic differences between

Table 1. Mean parameters and uncertainties as a function of $\alpha_{\rm ml}$ prior for KIC 3632418 to KIC 6603624. Bold font indicates the prior for which the highest evidence was obtained, as well as other priors for which the evidence was comparable (within a factor of 5). Y_0, Z_0: initial helium and metal mass fractions; $Z_{\rm s}$: metal mass fraction in the envelope; $R_{\rm BCZ}$: fractional radius of the base of the convection zone; $\alpha_{\rm ml}$: mixing length parameter; Sys: the most probable systematic-error model is given (SSE = standard surface effect, ASE = arbitrary systematic errors, NSE = no systematic errors) and asterisks indicate a probability contrast of less than an order of magnitude with respect to any of the other systematic-error models.

Star	α prior	$M/{\rm M}_\odot$	$\log T_{\rm eff}$	$\log L/{\rm L}_\odot$	$\log R/{\rm R}_\odot$	Age	Y_0	Z_0	$Z_{\rm s}$	$Z_{\rm s}/X_{\rm s}$	$R_{\rm BCZ}$	$\alpha_{\rm ml}$	Sys
3632418	**$\alpha_{\rm ml} = 1.8$**	1.273	3.802	0.696	0.268	3.926	0.252	0.0134	0.0130	0.0175	0.8397	1.80	SSE
		±0.033	±0.002	±0.007	±0.004	±0.227	±0.012	±0.0024	±0.0022	±0.0030	±0.0069		
	Gaussian	1.261	3.805	0.706	0.266	3.823	0.260	0.0130	0.0126	0.0172	0.8405	1.87	SSE
		±0.030	±0.003	±0.012	±0.004	±0.221	±0.024	±0.0025	±0.0022	±0.0033	±0.0088	±0.05	
	no $\alpha_{\rm ml}$ prior	1.264	3.807	0.713	0.266	3.738	0.264	0.0133	0.0129	0.0177	0.8386	1.91	SSE
		±0.029	±0.003	±0.012	±0.004	±0.217	±0.024	±0.0024	±0.0021	±0.0032	±0.0093	±0.06	
3656476	$\alpha_{\rm ml} = 1.8$	1.131	3.754	0.219	0.126	6.623	0.281	0.0310	0.0273	0.0373	0.6874	1.80	SSE
		±0.025	±0.004	±0.017	±0.003	±0.729	±0.011	±0.0028	±0.0026	±0.0038	±0.0090		
	Gaussian	1.159	3.754	0.230	0.130	6.871	0.276	0.0347	0.0308	0.0422	0.6732	1.94	SSE
		±0.022	±0.004	±0.017	±0.003	±0.564	±0.012	±0.0034	±0.0031	±0.0045	±0.0089	±0.07	
	no $\alpha_{\rm ml}$ prior	1.253	3.766	0.301	0.143	7.789	0.234	0.0400	0.0359	0.0473	0.6591	2.39	NSE*
		±0.013	±0.002	±0.007	±0.002	±0.287	±0.010	±0.0005	±0.0005	±0.0010	±0.0015	±0.02	
4914923	$\alpha_{\rm ml} = 1.8$	1.228	3.759	0.297	0.154	5.409	0.259	0.0306	0.0271	0.0361	0.7097	1.80	SSE
		±0.036	±0.003	±0.013	±0.004	±0.349	±0.021	±0.0017	±0.0016	±0.0025	±0.0078		
	Gaussian	1.227	3.764	0.314	0.153	5.269	0.263	0.0299	0.0266	0.0357	0.7075	1.88	SSE
		±0.037	±0.004	±0.018	±0.004	±0.446	±0.021	±0.0018	±0.0017	±0.0026	±0.0092	±0.05	
	no $\alpha_{\rm ml}$ prior	1.245	3.769	0.343	0.157	6.802	0.242	0.0337	0.0302	0.0399	0.6812	2.19	SSE
		±0.025	±0.005	±0.021	±0.003	±0.766	±0.020	±0.0035	±0.0032	±0.0044	±0.0102	±0.12	
5184732	$\alpha_{\rm ml} = 1.8$	1.239	3.761	0.261	0.132	4.421	0.277	0.0394	0.0350	0.0483	0.7258	1.80	SSE*
		±0.024	±0.005	±0.023	±0.003	±0.594	±0.008	±0.0016	±0.0015	±0.0023	±0.0143		
	Gaussian	1.253	3.764	0.278	0.135	4.951	0.271	0.0400	0.0360	0.0497	0.6995	2.03	SSE
		±0.022	±0.004	±0.020	±0.003	±0.370	±0.010	±0.0004	±0.0004	±0.0009	±0.0070	±0.06	
	no $\alpha_{\rm ml}$ prior	1.274	3.771	0.312	0.137	4.521	0.273	0.0399	0.0362	0.0502	0.7022	2.15	SSE
		±0.016	±0.003	±0.016	±0.002	±0.257	±0.008	±0.0007	±0.0006	±0.0011	±0.0049	±0.05	

Table 1 – *continued*

Star	α prior	$M/\mathrm{M}_\odot$	$\log T_{\rm eff}$	$\log L/\mathrm{L}_\odot$	$\log R/\mathrm{R}_\odot$	Age	Y_0	Z_0	$Z_{\rm s}$	$Z_{\rm s}/X_{\rm s}$	$R_{\rm BCZ}$	$\alpha_{\rm ml}$	Sys
5512589	**$\alpha_{\rm ml} = 1.8$**	1.106	3.756	0.408	0.216	7.843	0.272	0.0222	0.0192	0.0256	0.6620	1.80	SSE
		±0.031	±0.002	±0.008	±0.004	±0.303	±0.018	±0.0026	±0.0024	±0.0036	±0.0051		
	Gaussian	1.111	3.757	0.414	0.217	7.722	0.272	0.0223	0.0194	0.0259	0.6629	1.82	SSE
		±0.033	±0.003	±0.015	±0.004	±0.408	±0.019	±0.0026	±0.0024	±0.0036	±0.0054	±0.04	
	no $\alpha_{\rm ml}$ prior	1.117	3.758	0.421	0.218	7.588	0.272	0.0225	0.0196	0.0261	0.6640	1.84	SSE
		±0.034	±0.004	±0.019	±0.004	±0.472	±0.019	±0.0026	±0.0025	±0.0037	±0.0057	±0.05	
6106415	$\alpha_{\rm ml} = 1.8$	1.184	3.772	0.243	0.101	4.536	0.243	0.0236	0.0204	0.0264	0.7446	1.80	SSE
		±0.022	±0.004	±0.014	±0.003	±0.383	±0.014	±0.0023	±0.0021	±0.0029	±0.0088		
	Gaussian	1.264	3.772	0.264	0.112	4.939	0.224	0.0300	0.0265	0.0341	0.7174	2.06	NSE
		±0.012	±0.002	±0.010	±0.001	±0.170	±0.005	±< 0.0001	±0.0001	±0.0002	±0.0038	±0.05	
	no $\alpha_{\rm ml}$ prior	1.267	3.774	0.271	0.112	4.922	0.223	0.0299	0.0265	0.0340	0.7163	2.10	NSE*
		±0.007	±0.002	±0.008	±0.001	±0.150	±0.005	±0.0008	±0.0007	±0.0009	±0.0029	±0.02	
6116048	$\alpha_{\rm ml} = 1.8$	1.090	3.772	0.241	0.099	6.608	0.239	0.0159	0.0132	0.0166	0.7290	1.80	ASE
		±0.014	±0.003	±0.011	±0.002	±0.420	±0.009	±0.0019	±0.0017	±0.0023	±0.0073		
	Gaussian	1.066	3.763	0.200	0.097	9.328	0.237	0.0200	0.0167	0.0212	0.6747	2.01	SSE
		±0.022	±0.004	±0.019	±0.003	±0.763	±0.008	±0.0003	±0.0003	±0.0004	±0.0082	±0.04	
	no $\alpha_{\rm ml}$ prior	1.082	3.770	0.230	0.099	8.650	0.238	0.0197	0.0166	0.0212	0.6789	2.12	SSE
		±0.027	±0.005	±0.024	±0.004	±0.865	±0.009	±0.0012	±0.0010	±0.0013	±0.0100	±0.06	
6603624	$\alpha_{\rm ml} = 1.8$	1.052	3.735	0.029	0.067	9.830	0.264	0.0356	0.0301	0.0403	0.6625	1.80	SSE
		±0.022	±0.004	±0.015	±0.003	±0.708	±0.016	±0.0040	±0.0034	±0.0050	±0.0057		
	Gaussian	1.117	3.742	0.074	0.076	9.309	0.243	0.0373	0.0319	0.0418	0.6627	1.98	SSE*
		±0.028	±0.004	±0.017	±0.004	±0.593	±0.015	±0.0029	±0.0026	±0.0038	±0.0043	±0.05	
	no $\alpha_{\rm ml}$ prior	1.192	3.751	0.129	0.086	8.321	0.219	0.0371	0.0321	0.0411	0.6687	2.16	NSE*
		±0.013	±0.005	±0.018	±0.002	±0.290	±0.005	±0.0025	±0.0021	±0.0027	±0.0016	±0.05	
6933899	$\alpha_{\rm ml} = 1.8$	1.164	3.756	0.393	0.208	7.808	0.248	0.0245	0.0212	0.0275	0.6779	1.80	ASE
		±0.047	±0.004	±0.022	±0.006	±0.571	±0.018	±0.0021	±0.0020	±0.0028	±0.0154		
	Gaussian	1.140	3.760	0.401	0.205	7.806	0.259	0.0237	0.0207	0.0273	0.6650	1.90	ASE
		±0.064	±0.004	±0.027	±0.008	±0.620	±0.024	±0.0026	±0.0024	±0.0033	±0.0189	±0.05	
	no $\alpha_{\rm ml}$ prior	1.131	3.766	0.426	0.204	7.553	0.265	0.0223	0.0196	0.0260	0.6589	2.04	ASE*
		±0.053	±0.005	±0.028	±0.007	±0.574	±0.022	±0.0027	±0.0025	±0.0035	±0.0146	±0.09	
7680114	$\alpha_{\rm ml} = 1.8$	1.156	3.761	0.309	0.157	6.084	0.286	0.0294	0.0259	0.0355	0.7012	1.80	SSE
		±0.025	±0.003	±0.010	±0.003	±0.544	±0.009	±0.0018	±0.0017	±0.0025	±0.0068		
	Gaussian	1.172	3.766	0.333	0.159	5.780	0.284	0.0289	0.0256	0.0351	0.7004	1.89	SSE
		±0.027	±0.004	±0.017	±0.003	±0.567	±0.010	±0.0022	±0.0020	±0.0030	±0.0076	±0.05	
	no $\alpha_{\rm ml}$ prior	1.186	3.771	0.356	0.160	5.521	0.284	0.0281	0.0251	0.0345	0.6997	1.99	SSE
		±0.033	±0.005	±0.024	±0.004	±0.721	±0.011	±0.0025	±0.0023	±0.0034	±0.0101	±0.08	
8006161	$\alpha_{\rm ml} = 1.8$	1.052	3.721	−0.207	−0.022	2.714	0.265	0.0395	0.0377	0.0532	0.6891	1.80	SSE
		±0.022	±0.003	±0.010	±0.003	±0.500	±0.015	±0.0015	±0.0015	±0.0026	±0.0026		
	Gaussian	1.077	3.721	−0.201	−0.019	3.220	0.246	0.0398	0.0378	0.0519	0.6847	1.91	SSE
		±0.027	±0.003	±0.011	±0.004	±0.541	±0.020	±0.0010	±0.0009	±0.0019	±0.0037	±0.07	
	no $\alpha_{\rm ml}$ prior	1.114	3.721	−0.188	−0.013	3.896	0.219	0.0400	0.0377	0.0499	0.6791	2.10	SSE
		±0.017	±0.003	±0.011	±0.002	±0.453	±0.011	±0.0003	±0.0003	±0.0008	±0.0024	±0.06	
8228742	$\alpha_{\rm ml} = 1.8$	1.214	3.762	0.518	0.260	6.584	0.240	0.0200	0.0174	0.0224	0.6906	1.80	SSE
		±0.021	±0.002	±0.002	±0.003	±0.200	±0.014	±0.0003	±0.0003	±0.0005	±0.0025		
	Gaussian	1.248	3.771	0.565	0.264	5.868	0.241	0.0199	0.0175	0.0225	0.6996	1.95	SSE
		±0.025	±0.004	±0.017	±0.003	±0.259	±0.012	±0.0006	±0.0006	±0.0008	±0.0038	±0.05	
	no $\alpha_{\rm ml}$ prior	1.274	3.778	0.596	0.266	5.479	0.240	0.0199	0.0175	0.0225	0.7047	2.05	SSE
		±0.027	±0.004	±0.017	±0.003	±0.261	±0.014	±0.0006	±0.0006	±0.0008	±0.0039	±0.06	
8379927	$\alpha_{\rm ml} = 1.8$	1.253	3.774	0.184	0.068	1.513	0.226	0.0250	0.0237	0.0310	0.7638	1.80	NSE*
		±0.011	±0.001	±0.007	±0.001	±0.231	±0.003	±0.0003	±0.0003	±0.0005	±0.0039		
	Gaussian	1.258	3.778	0.201	0.068	1.511	0.227	0.0246	0.0233	0.0305	0.7651	1.86	NSE*
		±0.016	±0.004	±0.018	±0.002	±0.248	±0.004	±0.0014	±0.0014	±0.0019	±0.0044	±0.06	
	no $\alpha_{\rm ml}$ prior	1.262	3.797	0.279	0.069	1.624	0.231	0.0204	0.0191	0.0249	0.7750	2.18	NSE*
		±0.017	±0.007	±0.029	±0.002	±0.231	±0.004	±0.0014	±0.0014	±0.0019	±0.0060	±0.13	
8760414	**$\alpha_{\rm ml} = 1.8$**	0.839	3.775	0.084	0.016	11.400	0.245	0.0050	0.0038	0.0046	0.7212	1.80	SSE
		±0.013	±0.002	±0.014	±0.002	±0.873	±0.002	±< 0.0001	±< 0.0001	±< 0.0001	±0.0090		
	Gaussian	0.838	3.775	0.084	0.016	11.426	0.245	0.0050	0.0038	0.0046	0.7209	1.80	SSE
		±0.013	±0.002	±0.014	±0.002	±0.886	±0.002	±< 0.0001	±< 0.0001	±< 0.0001	±0.0092	±0.02	

Table 1 – *continued*

Star	α prior	$M/M_\odot$	$\log T_{\rm eff}$	$\log L/L_\odot$	$\log R/R_\odot$	Age	Y_0	Z_0	$Z_{\rm s}$	$Z_{\rm s}/X_{\rm s}$	$R_{\rm BCZ}$	$\alpha_{\rm ml}$	Sys
	no $\alpha_{\rm ml}$ prior	0.862	3.789	0.147	0.020	10.511	0.245	0.0050	0.0039	0.0048	0.7181	2.25	SSE
		±0.015	±0.008	±0.037	±0.003	±0.706	±0.001	±<0.0001	±<0.0001	±0.0001	±0.0049	±0.26	
10516096	$\alpha_{\rm ml} = 1.8$	1.185	3.765	0.338	0.163	6.049	0.258	0.0244	0.0213	0.0280	0.7128	1.80	NSE
		±0.017	±0.002	±0.009	±0.002	±0.461	±0.016	±0.0016	±0.0016	±0.0024	±0.0060		
	Gaussian	1.210	3.772	0.374	0.166	5.854	0.247	0.0229	0.0201	0.0261	0.7160	1.92	NSE
		±0.021	±0.004	±0.020	±0.003	±0.533	±0.019	±0.0025	±0.0023	±0.0034	±0.0079	±0.06	
	no $\alpha_{\rm ml}$ prior	1.240	3.781	0.419	0.170	5.500	0.238	0.0213	0.0189	0.0243	0.7188	2.11	NSE
		±0.018	±0.005	±0.022	±0.002	±0.500	±0.013	±0.0022	±0.0020	±0.0028	±0.0072	±0.09	
10963065	$\alpha_{\rm ml} = 1.8$	1.122	3.778	0.259	0.097	5.035	0.252	0.0174	0.0147	0.0189	0.7511	1.80	SSE
		±0.037	±0.005	±0.025	±0.005	±0.945	±0.018	±0.0025	±0.0023	±0.0032	±0.0167		
	Gaussian	1.094	3.777	0.248	0.094	6.139	0.252	0.0176	0.0148	0.0191	0.7254	1.92	SSE
		±0.038	±0.005	±0.026	±0.005	±1.090	±0.18	±0.0025	±0.0022	±0.0032	±0.0198	±0.07	
	no $\alpha_{\rm ml}$ prior	1.089	3.785	0.278	0.093	6.538	0.245	0.0154	0.0129	0.0165	0.7162	2.15	SSE
		±0.029	±0.005	±0.026	±0.004	±0.846	±0.012	±0.0013	±0.0012	±0.0017	±0.0135	±0.09	
11244118	$\alpha_{\rm ml} = 1.8$	1.233	3.751	0.392	0.218	7.100	0.265	0.0388	0.0345	0.0470	0.6830	1.80	SSE
		±0.053	±0.007	±0.038	±0.006	±1.232	±0.014	±0.0026	±0.0025	±0.0036	±0.0267		
	Gaussian	1.299	3.752	0.412	0.227	7.633	0.231	0.0400	0.0359	0.0471	0.6557	2.01	NSE*
		±0.004	±0.002	±0.008	±0.000	±0.222	±0.005	±0.0001	±0.0001	±0.0004	±0.0017	±0.03	
	no $\alpha_{\rm ml}$ prior	1.291	3.759	0.438	0.226	6.962	0.247	0.0400	0.0360	0.0483	0.6603	2.09	NSE*
		±0.004	±0.003	±0.011	±0.000	±0.292	±0.007	±< 0.0001	±0.0001	±0.0005	±0.0021	±0.04	
11713510	**$\alpha_{\rm ml} = 1.8$**	1.025	3.772	0.441	0.200	7.135	0.291	0.0139	0.0115	0.0153	0.6992	1.80	SSE
		±0.019	±0.003	±0.013	±0.003	±0.508	±0.019	±0.0022	±0.0019	±0.0028	±0.0121		
	Gaussian	1.031	3.773	0.447	0.201	7.042	0.294	0.0145	0.0121	0.0162	0.6930	1.85	SSE
		±0.022	±0.003	±0.013	±0.003	±0.424	±0.017	±0.0019	±0.0017	±0.0025	±0.0121	±0.05	
	no $\alpha_{\rm ml}$ prior	1.082	3.775	0.467	0.208	6.705	0.290	0.0182	0.0157	0.0213	0.6829	1.99	SSE*
		±0.071	±0.003	±0.025	±0.010	±0.522	±0.016	±0.0057	±0.0055	±0.0077	±0.0138	±0.15	
12009504	$\alpha_{\rm ml} = 1.8$	1.238	3.773	0.360	0.157	4.558	0.252	0.0239	0.0207	0.0270	0.7451	1.80	SSE
		±0.034	±0.003	±0.017	±0.004	±0.488	±0.019	±0.0021	±0.0019	±0.0028	±0.0122		
	Gaussian	1.245	3.779	0.386	0.158	4.487	0.250	0.0223	0.0195	0.0253	0.7419	1.93	SSE
		±0.028	±0.004	±0.018	±0.003	±0.480	±0.018	±0.0025	±0.0022	±0.0033	±0.0112	±0.05	
	no $\alpha_{\rm ml}$ prior	1.253	3.786	0.416	0.159	4.332	0.249	0.0205	0.0180	0.0234	0.7410	2.07	SSE
		±0.026	±0.005	±0.021	±0.003	±0.367	±0.016	±0.0016	±0.0014	±0.0021	±0.0103	±0.08	
12258514	$\alpha_{\rm ml} = 1.8$	1.250	3.769	0.440	0.206	5.564	0.250	0.0256	0.0224	0.0294	0.7291	1.80	SSE
		±0.039	±0.004	±0.020	±0.004	±0.939	±0.018	±0.0021	±0.0019	±0.0028	±0.0137		
	Gaussian	1.227	3.769	0.436	0.204	6.342	0.246	0.0255	0.0225	0.0293	0.7086	1.90	SSE
		±0.038	±0.003	±0.017	±0.004	±0.823	±0.019	±0.0024	±0.0023	±0.0035	±0.0138	±0.04	
	no $\alpha_{\rm ml}$ prior	1.217	3.771	0.445	0.203	6.445	0.245	0.0242	0.0213	0.0278	0.7046	1.96	SSE
		±0.041	±0.004	±0.020	±0.005	±0.701	±0.018	±0.0029	±0.0027	±0.0039	±0.0134	±0.06	
16 Cyg A	$\alpha_{\rm ml} = 1.8$	1.054	3.762	0.173	0.086	6.441	0.291	0.0250	0.0214	0.0291	0.7027	1.80	SSE
		±0.010	±0.001	±0.006	±0.001	±0.363	±0.006	±< 0.0001	±0.0002	±0.0004	±0.0036		
	Gaussian	1.095	3.765	0.196	0.092	7.055	0.280	0.0281	0.0247	0.0337	0.6730	2.13	SSE
		±0.016	±0.005	±0.023	±0.002	±0.375	±0.012	±0.0024	±0.0021	±0.0033	±0.0056	±0.06	
	no $\alpha_{\rm ml}$ prior	1.114	3.771	0.225	0.095	6.647	0.269	0.0250	0.0220	0.0295	0.6795	2.20	SSE
		±0.009	±0.001	±0.004	±0.001	±0.206	±0.006	±0.0003	±0.0002	±0.0005	±0.0015	±0.01	
16 Cyg B	$\alpha_{\rm ml} = 1.8$	1.007	3.758	0.070	0.043	6.464	0.294	0.0247	0.0214	0.0294	0.6986	1.80	SSE
		±0.006	±0.002	±0.007	±0.001	±0.250	±0.004	±0.0012	±0.0010	±0.0015	±0.0035		
	Gaussian	1.023	3.762	0.091	0.045	6.532	0.289	0.0250	0.0217	0.0296	0.6942	1.92	SSE
		±0.013	±0.002	±0.010	±0.002	±0.281	±0.007	±0.0001	±0.0001	±0.0003	±0.0034	±0.04	
	no $\alpha_{\rm ml}$ prior	1.076	3.764	0.116	0.054	9.279	0.234	0.0250	0.0214	0.0274	0.6621	2.40	SSE
		±0.012	±0.002	±0.009	±0.002	±0.473	±0.005	±0.0001	±0.0001	±0.0003	±0.0035	±0.00	
Kepler-36	**$\alpha_{\rm ml} = 1.8$**	1.113	3.771	0.475	0.220	6.923	0.256	0.0150	0.0124	0.0159	0.7059	1.80	NSE
		±0.035	±0.003	±0.015	±0.005	±0.372	±0.018	±0.0004	±0.0004	±0.0006	±0.0121		
	Gaussian	1.118	3.771	0.480	0.221	6.870	0.255	0.0150	0.0125	0.0159	0.7058	1.82	NSE
		±0.035	±0.003	±0.017	±0.005	±0.386	±0.018	±0.0004	±0.0004	±0.0006	±0.0122	±0.04	
	no $\alpha_{\rm ml}$ prior	1.123	3.773	0.486	0.222	6.792	0.254	0.0150	0.0125	0.0160	0.7058	1.85	NSE
		±0.036	±0.004	±0.021	±0.005	±0.409	±0.018	±0.0004	±0.0004	±0.0006	±0.0122	±0.06	

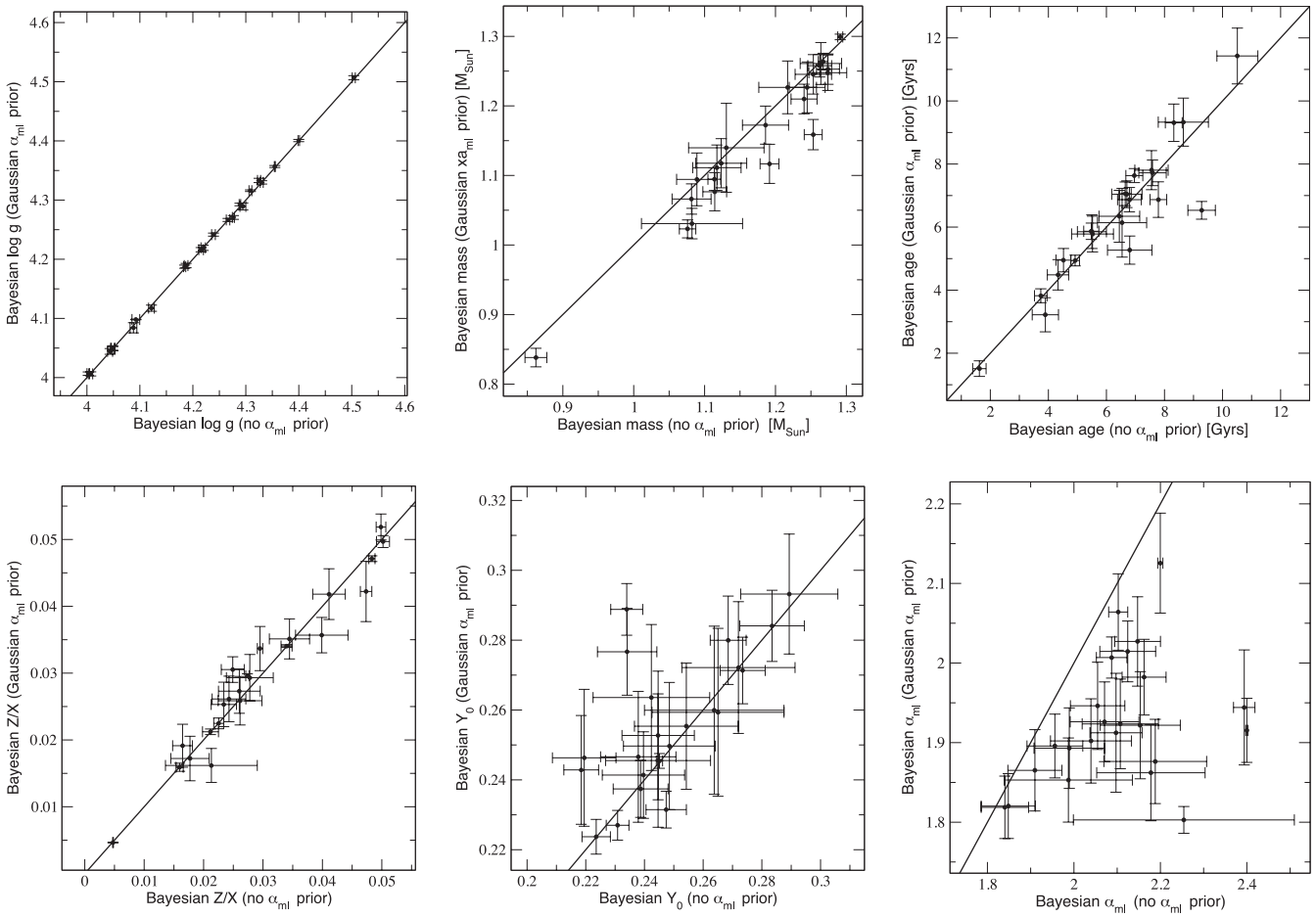

Figure 4. The effect of the Gaussian $\alpha_{\rm ml}$ prior on the posterior value of various model parameters. Results are plotted for the most probable systematic error model as given in e.g. Table 1. The black line indicates a ratio of unity.

the Gaussian prior and the $\alpha_{\rm ml} = 1.8$ prior results are smaller than those obtained in a comparison without any priors on $\alpha_{\rm ml}$. Overall, our comparison reveals that stronger constraints on $\alpha_{\rm ml}$ do not perturb the parameters outside the uncertainties and produce slightly lower stellar masses and higher Y_0.

In terms of the systematic errors, in particular the surface effect, the results also follow our conclusions from the previous section. Fig. 6 shows the differences in the systematic errors that arise by using the two $\alpha_{\rm ml}$ priors for every mode of every star in our sample. Using the Gaussian $\alpha_{\rm ml}$ prior leads to an increase in the magnitude of the surface effects (= more negative systematic differences between observed and calculated frequencies) in general. There are only a few stars in the sample for which the effect is very pronounced. It is interesting that for many modes the Gaussian $\alpha_{\rm ml}$ prior does not produce large differences for the surface effects. This is due to the fact that we find a number of stars for which the surface effects are not significant unless we restrict the analysis to the $\alpha_{\rm ml} = 1.8$ models. Consequently, switching to the $\alpha_{\rm ml} = 1.8$ prior results in even bigger surface effects and to significant surface effects for more stars in the sample. This is also reflected in the strong preference for the SSE model, as shown in the result tables. In both panels there are also a few outliers for which the priors lead to decreased surface effects (= more positive systematic differences between observed and calculated frequencies), but these modes belong to the stars for which the ASE model is either preferred or very similar in probability to the surface effect model.

As indicated in our result tables, using no $\alpha_{\rm ml}$ prior often leads to the highest evidence. Larger evidence values require that the models are formally more consistent with all our available constraints while also minimizing the systematic errors, i.e. the surface effects. Therefore, the analysis which yields the highest evidence and thus the corresponding stellar parameters are usually interpreted as being most appropriate. As explained in Section 3, however, we stress that at this point it is necessary to present the results from all approaches, and not to put too much confidence into the formal preference over to $\alpha_{\rm ml}$ priors. This follows simply because we do not possess enough low-order modes or additional information to anchor the surface effect relation. The only clear exception to this are KIC 8379927 and KIC 10516096, for which we do not detect significant systematic errors irrespective of the $\alpha_{\rm ml}$ priors but still find higher $\alpha_{\rm ml}$ to be most probable. Concerning the impact of $\alpha_{\rm ml}$ on the other stellar parameters, however, only the stellar mass and Y_0 seem to be somewhat systematically affected by the choice of priors. Even for those parameters the deviations are usually within the quoted uncertainties. Thus, for our comparison with the values published in the literature, which also allow different values of $\alpha_{\rm ml}$, we constrain ourselves to the results obtained using the 'intermediate approach', the Gaussian $\alpha_{\rm ml}$ prior and refer to our tabulated results for the differences arising from the different priors.

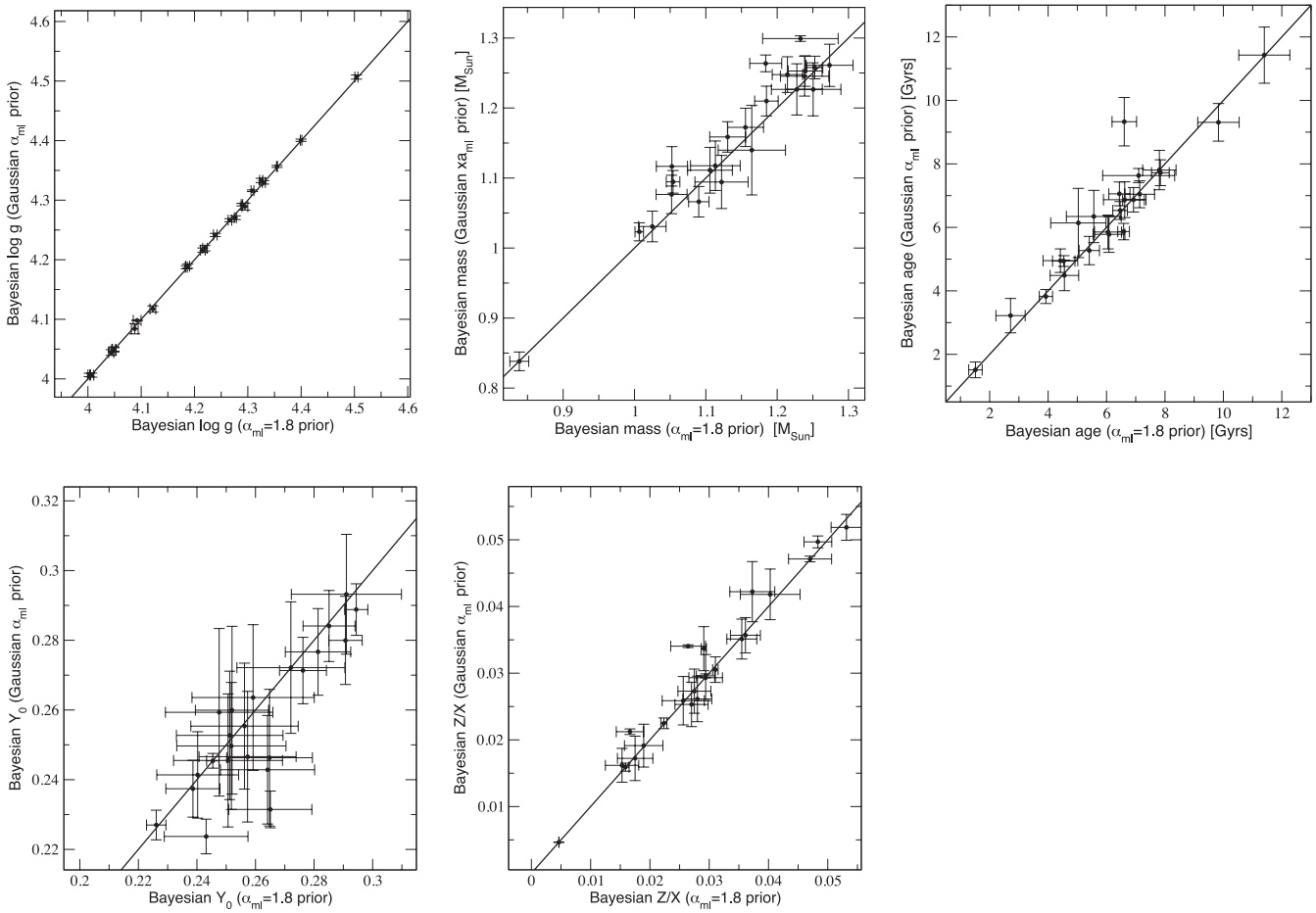

Figure 5. Same as Fig. 4 but for the $\alpha_{\rm ml} = 1.8$ prior and the Gaussian $\alpha_{\rm ml}$ prior. Comparison of $\alpha_{\rm ml}$ is not shown.

4.2 Surface effects and other systematic frequency differences

As previously alluded to, Fig. 6 suggests that many stars do not show strong evidence for surface effects when our non-adiabatic models are used in tandem with the Gaussian prior. The situation changes, however, when the $\alpha_{\rm ml} = 1.8$ prior is used. This implies that, depending on the prior, the convective contributions to the surface effects are either more or less significant. Since a proper normalization of the surface effect amplitudes is not trivial and the shape of the surface effects can vary from star to star, we instead quantify the significance of the surface effect in terms of probabilities. As discussed in Section 2.3, our calculations consider three different systematic error models: SSE, ASE and NSE. Therefore, in order to quantify the surface effect significance for every star, we simply calculate the odds ratio

$$\mathrm{ODDS} = \frac{\mathrm{ev(SSE)}}{\mathrm{ev(ASE)} + \mathrm{ev(NSE)}}, \tag{5}$$

where ev(SSE), ev(ASE) and ev(NSE) are the evidence values obtained for the analysis using each specific systematic error model.[7] This is the probability ratio between the hypotheses 'SSE' and 'either ASEs or no systematic errors'. Therefore, if surface effects are needed to explain the observations, we expect that ODDS $\gg 1$. According to the convention established by Jeffreys (1961), the evidence for or against one of the two hypotheses is considered 'substantial' for a factor of 3–10, 'strong' for a factor of 10–30, 'very strong' for a factor of 30–100 and 'decisive' for factors above 100. Hence, when the surface effects become more significant with respect to the other hypotheses, ODDS will increase as well.

Our calculations show that for some stars the significance of the individual systematic error models depend on the specific prior for $\alpha_{\rm ml}$, in accordance with what was discussed in Section 3. However, there are four stars for which ODDS < 1 irrespective of mixing length parameter: KIC 6933899, KIC 8379927, KIC 10516096 and Kepler-36. The latter three objects do not require any systematic errors at all. Furthermore, for KIC 6106415, KIC 6603624 and KIC 11244118 the surface effect model is only significant for the $\alpha_{\rm ml} = 1.8$ prior.

Fig. 7 shows the actual systematic error measurements obtained when using the Gaussian $\alpha_{\rm ml}$ prior that have been rescaled and plotted as a function of their mean $\alpha_{\rm ml}$. For many stars the individual deviations do not seem to correspond to the clear power-law behaviour that can be identified for the Sun. Furthermore, there appears to be a very weak dependence on $\alpha_{\rm ml}$, where higher values are related to smaller normalized surface effects, as expected from the discussion in Section 3. Whether this dependence is physically meaningful depends on whether these stars actually have higher values of $\alpha_{\rm ml}$, or if it is simply the case that our $\alpha_{\rm ml}$ prior is too weak. In any case, $\alpha_{\rm ml}$ and surface effects are related.

Similar to Mathur20, we do not find any simple correlations of the normalized surface effect with any of the other parameters in

[7] This assumes that a priori all three surface effect models are equally probable.

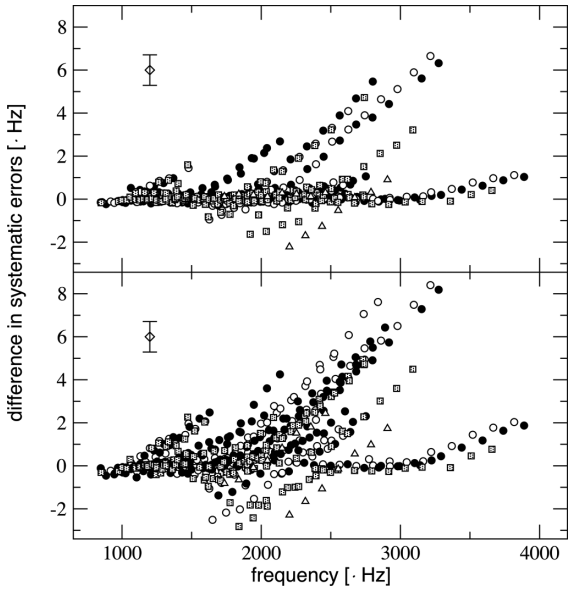

Figure 6. Differences in the measured systematic errors that arise from using the Gaussian $\alpha_{\rm ml}$ prior (top panel) or the $\alpha_{\rm ml} = 1.8$ prior (bottom panel). All modes of all stars are shown: $l = 0$ modes (open circles), $l = 1$ modes (black circles), $l = 2$ modes (shaded squares) and $l = 3$ modes (open triangles). Positive (negative) values denote bigger (smaller) systematic errors in terms of surface effects when the $\alpha_{\rm ml}$ priors are used. The average uncertainty of the differences is indicated by the diamond in the upper left. For each star, the plotted differences were obtained using the most probable systematic difference model for the respective $\alpha_{\rm ml}$ prior.

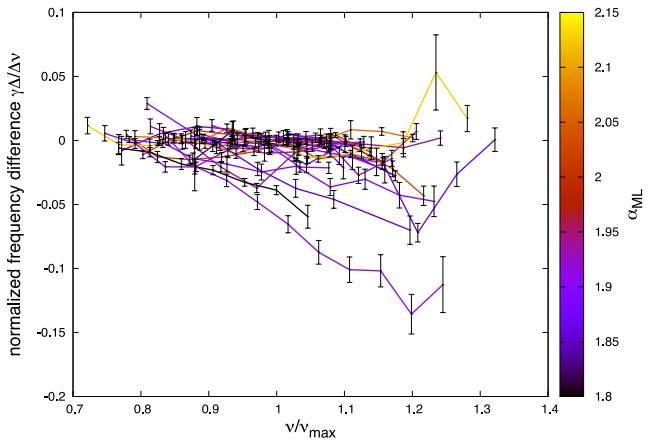

Figure 7. Normalized systematic frequency differences as a function of normalized frequency for $l = 0$ modes for the results obtained with the Gaussian $\alpha_{\rm ml}$ prior. The colour represents the mean posterior $\alpha_{\rm ml}$. For each star, the plotted differences were obtained using the most probable systematic difference model.

Table 1. However, studying the *significance* of the surface effect in terms of probabilities reveals some interesting results. Fig. 8 shows the logarithm of the odds ratio for all stars in our sample as a function of their position in the HR diagram. The most significant detections appear to be situated at close-to-solar values of $T_{\rm eff}$ and the picture is similar whether the Gaussian $\alpha_{\rm ml}$ prior, the $\alpha_{\rm ml} = 1.8$ prior or no $\alpha_{\rm ml}$ prior is used. Furthermore, the coolest star in the sample, KIC 8006161, also displays highly significant surface effects but lies far off from the main bulk of the sample. We have also added symbols representing the Sun (Gruberbauer & Guenther 2013),

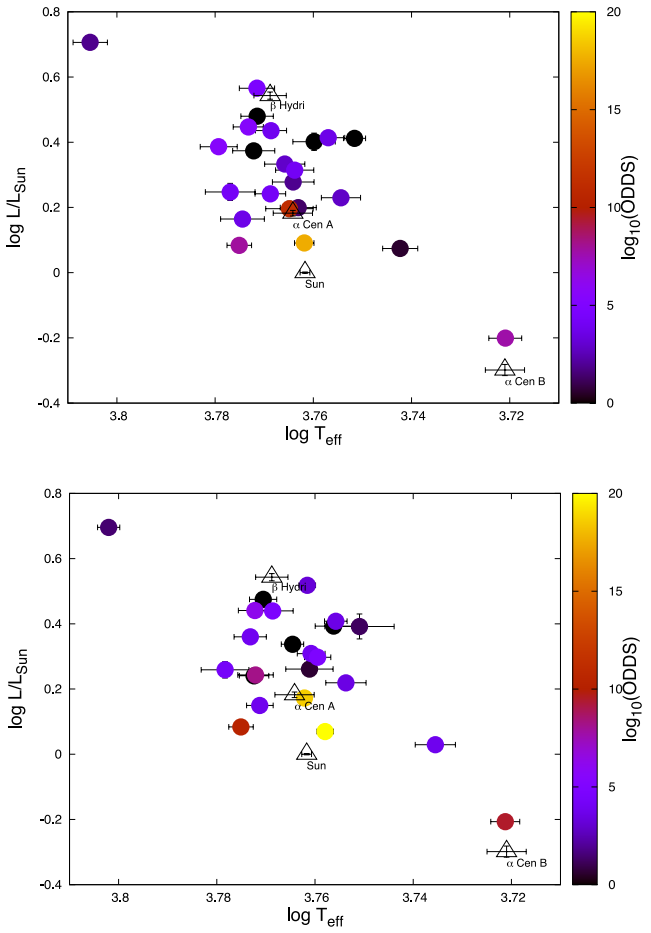

Figure 8. HR diagram of all stars in our sample (filled circles) with parameter taken from Table 1, using the results from the Gaussian (top panel) and $\alpha_{\rm ml} = 1.8$ (bottom panel) prior. The colour indicates the significance of the detected surface effect using $\log_{10}$(ODDS). Four other well-known stars with surface effects are also shown as triangles. For each star, the plotted parameters were obtained using the most probable systematic difference model for the respective $\alpha_{\rm ml}$ prior.

β Hydri (Brandão et al. 2011) and α Cen A & B (Eggenberger et al. 2004), all of which were used by Kjeldsen et al. (2008) to define the surface effect correction. Except for β Hydri,[8] the stars fit well into the pattern given by the *Kepler* stars. 16 Cyg A, 16 Cyg B, α Cen A and of course the Sun, appear to lie on the 'surface effect locus' in the HR diagram of our sample. α Cen B, on the other hand, is situated very close to KIC 800616.

The stars for which no significant surface effects were detected do mix with stars that show less significant detections, which is why there does not seem to be a strong correlation of the surface effect with any particular parameter. On average, however, lower luminosities and higher effective temperatures correspond to more significant surface effects. Plotting $\log T_{\rm eff}$ against $\log g$ (not shown) necessarily yields a very similar picture which again clusters the

[8] Note that the surface effects detected in β Hydri have only been measured using adiabatic frequencies which do not contain the correction for radiative gains and losses.

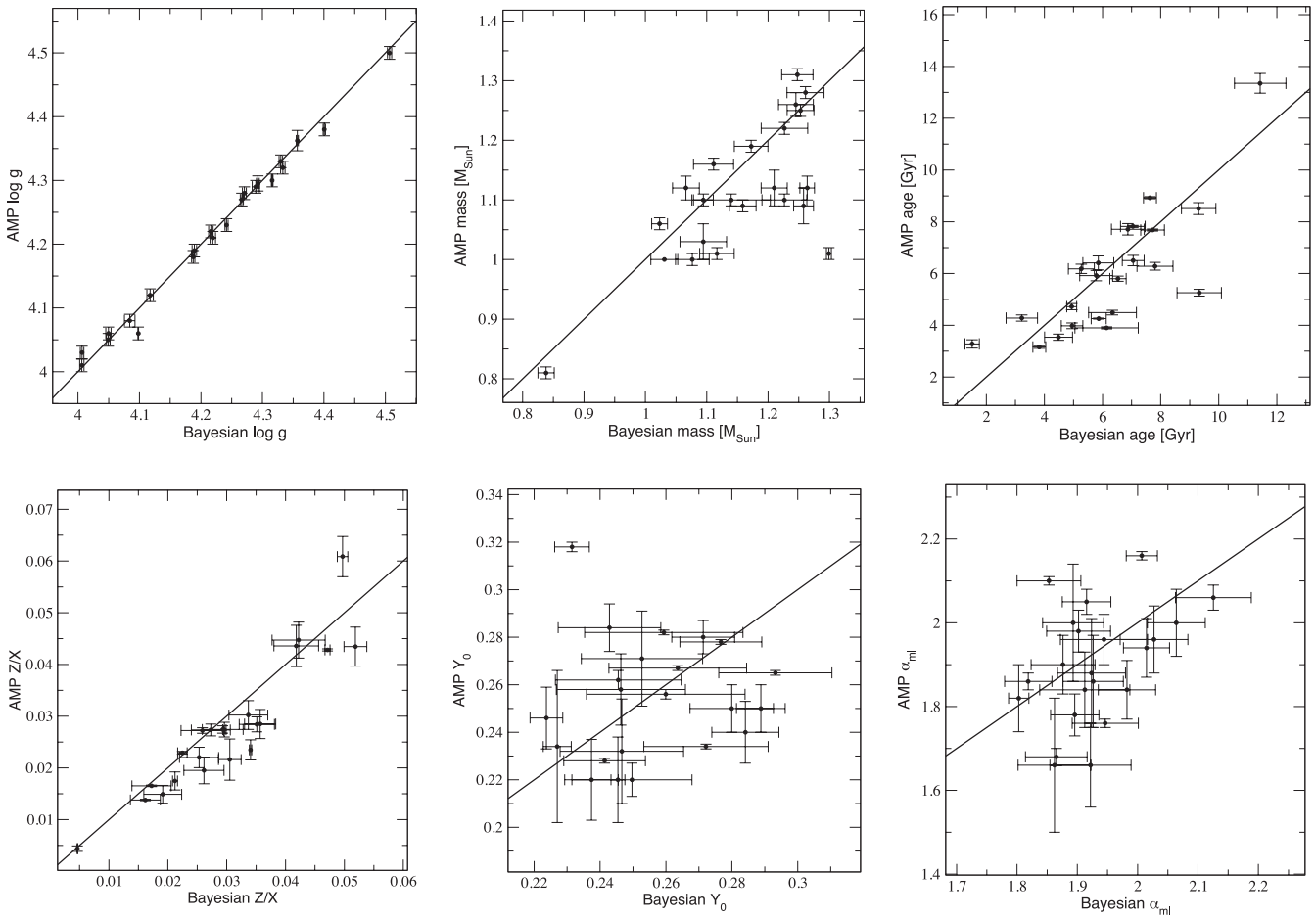

Figure 9. Same as Fig. 4 but comparing the results from our Bayesian approach using the $\alpha_{\rm ml}$ prior with the published results obtained via the AMP pipeline (Mathur20; Metcalfe et al. 2012). Note that Kepler-36 is not included in these plots.

most significant detections at the solar values. A correlation of the surface effect amplitude with $\log g$ was already noted by Mathur20. Our comparison of the significance of the surface effect would be more in line with their investigation of the normalized surface effect for which they could not find a strong correlation. It will be intriguing to see whether a bigger sample and additional lower order modes could lead to a clearer detection of a 'surface effect locus' in the HR diagram.

In any case, the non-detection of surface effects in some stars as well as the concentration of very significant surface effects for stars with close to solar values should be a warning for unreflected usage of the standard surface correction for all solar-like stars.

4.3 Comparison with non-Bayesian results

4.3.1 Mathur20

In this section we investigate the presence of potential systematic differences between our results and those obtained using the AMP pipeline. Fig. 9 shows that there are no strong systematic trends in either of the plotted parameters. As in the comparison between our three different Bayesian analyses (Figs 4 and 5), the determined $\log g$ values are very similar, but the Bayesian uncertainties are usually smaller. The results for $\alpha_{\rm ml}$ show large scatter which is mostly compensated by the large uncertainties. It should be noted that our grid only extends from $\alpha_{\rm ml} = 1.8$ to 2.4, and therefore we do not cover the lower values that AMP returns for some of the stars.

The masses that were determined are quite similar for most stars, but the AMP delivers smaller uncertainties on average. For several stars, only the larger uncertainties reported by the Bayesian method can help to reconcile the results. There exists also a clear outlier with KIC 11244118 where the masses differ by about 0.3 $M_\odot$, more than 15 times our statistical uncertainty.[9] The initial helium mass fraction again displays large but seemingly unsystematic scatter, in particular when compared to some of the uncertainties reported by AMP. Many of the stars appear to prefer very low values of Y_0, as was also found to be the case by Mathur20. However, for these stars our various approaches (different $\alpha_{\rm ml}$ priors, different systematic error models) can often provide a solution with higher values albeit lower evidence. Also, in many cases the Bayesian uncertainties are usually large enough to reconcile the values with those required from studies of big bang nucleosynthesis. The only clear outlier here is KIC 8379927 for which we find quite large disagreements with the AMP results. Contrary to the somewhat larger discrepancies for Y_0, the results for Z/X are more similar, but our values appear to

[9] This star is also problematic since it fits best to models near the border of our grid both in terms of mass and metallicity.

be slightly larger in a systematic way. In general, we have to stress that concerning the chemical composition, our grid is quite coarse compared to the capabilities of AMP's genetic algorithm.

Lastly, significant differences appear in the comparison of the determined ages. Irrespective of potential differences in the definition of zero-age models, the two methods yield different results with significant scatter. Moreover, the Bayesian age uncertainties appear to be bigger on average by a factor of 6, which is substantial, necessary, but insufficient to reconcile the results in many cases.

We re-emphasize that the Bayesian uncertainties are properly propagated through the whole grid and also include the effects of the systematic frequency differences (via marginalization) and any non-asteroseismic constraints (via the prior probabilities). AMP, on the other hand, can only consider statistical contributions to the uncertainties. While dependent on the particular grid that was analysed, the Bayesian uncertainties are therefore superior from a methodological point of view. This different approach, as well as differences in the stellar models themselves, is sufficient to explain the reported discrepancies.

4.3.2 16 Cyg A&B

The modelling performed by Metcalfe et al. (2012) revealed that 16 Cyg A&B are of slightly different masses but have a similar age, as expected for a binary system. Several different grids and methods were used, including AMP, to arrive at an average ensemble solution. Our results compare favourably with this ensemble average, when it comes to the ages, the masses, Z_0 and $\alpha_{\rm ml}$. Except for the mass of 16 Cyg B, for which we obtain $1.023 \pm 0.013\,{\rm M}_{\odot}$ compared to their result of $1.07 \pm 0.02\,{\rm M}_{\odot}$, these parameters overlap within their respective 1σ uncertainties. It should be noted that we obtain a lower mass for 16 Cyg A as well, which might suggest a systematic difference between the methods and models used. As discussed in the previous section, however, we do not find that such a trend is true for our larger sample. The ages are fully consistent with a common origin, even though this constraint was not used in the analysis.[10]

We find a slight discrepancy for the initial helium mass fraction. For 16 Cyg A we obtain $Y_0 = 0.282 \pm 0.01$ and for 16 Cyg B we find $Y_0 = 0.285 \pm 0.01$, while Metcalfe et al. report 0.25 ± 0.01. Overall, we observe that the differences between our results and the ensemble average in the literature are minor.

Comparing our results exclusively to the AMP values, we see a significant difference in the age and the value of $\alpha_{\rm ml}$ for 16 Cyg B. It is interesting that this star is among the set of the most significant surface-effect detections in our sample. As the AMP results in a value of $\alpha_{\rm ml} = 2.05 \pm 0.03$, which is bigger than the ensemble average, it is perhaps the combination of the solar-calibrated surface effect correction and the use of a higher than solar $\alpha_{\rm ml}$ which results in the discrepancy. For the age, we obtained 6.532 ± 0.281 Gyr compared to 5.8 ± 0.1. Consistent with our findings in Section 4.3.1, we observe that our age uncertainties are significantly bigger.

In a recent paper, White et al. (2013) have combined interferometric diameters from Center for High Angular Resolution Astronomy (CHARA) observations with *Hipparcos* parallaxes, spectrophotometric bolometric fluxes and the asteroseismic large frequency separation, to obtain largely model-independent constraints for 16 Cyg A&B. In comparison to their results, for 16 Cyg A, our $\alpha_{\rm ml} = 1.8$ prior produces a very close match in terms of mass and radius, but the model $T_{\rm eff}$ values are slightly too low and match better for the Gaussian $\alpha_{\rm ml}$ prior. For 16 Cyg B, on the other hand, the higher $\alpha_{\rm ml}$ values are more consistent with their results, predicting higher masses and larger radii but again $T_{\rm eff}$ values that are not quite high enough to match the mean observed values. These slight differences however are insignificant and, irrespective of the particular priors used, we find that our results match the masses, temperatures and radii from White et al. (2013) reasonably well and in all cases to within the combined 1.5σ uncertainties. Therefore, the interferometric uncertainties are too large to give strong evidence for or against our particular solutions (i.e. in particular the different $\alpha_{\rm ml}$ values). This can also be interpreted as additional justification for the various $\alpha_{\rm ml}$ priors, since the range of results allows us to define a parameter space that is more in line with model-independent observations.

[10] The equal age is in even better agreement with our results for the $\alpha_{\rm ml} = 1.8$ prior, but for this approach we also obtain substantially smaller masses.

4.3.3 Kepler-36

With respect to Kepler-36, we find that we can match all parameters published in Carter et al. (2012) within the uncertainties. It is interesting, however, that we do not detect any surface effects for this star. Carter et al. report that the surface-effect correction was applied to the frequencies. Judging from our results, any surface effects necessary to be corrected for this star would have to originate from the radiative losses that are already taken into account in our non-adiabatic models.

5 CONCLUSIONS

In this paper we have reported on our asteroseismic analysis of 23 previously published stars that were observed with the *Kepler* satellite. We compared the results obtained with our Bayesian grid-based method to the results from the literature, most importantly those obtained with the AMP. Except for a weak trend towards larger values of Z/X with our method, no obvious systematic differences in the basic stellar parameters can be found. In part, this is certainly due to spectroscopic constraints ($T_{\rm eff}$, $\log g$, [Fe/H], $L/{\rm L}_{\odot}$) that were used by all authors.

However, we observe that the uncertainties derived from the two methods differ substantially for some stellar parameters. Uncertainties in the stellar ages in particular are either significantly underestimated by AMP or significantly overestimated by the Bayesian method. We conclude that the flexible treatment of the surface effects in the Bayesian approach is probably responsible for this discrepancy. Different values of $\alpha_{\rm ml}$ and the usage of non-adiabatic models require a more flexible treatment of the surface effect. Therefore, in our view the uncertainties derived with our method more adequately represent our actual state of knowledge about the surface effects and are therefore more realistic. On the other hand, the interplay between the surface effect and $\alpha_{\rm ml}$ introduces another layer of complexity in the analysis which has to be taken into account in the determination of the stellar parameters. We propose that future studies with more stars should aim to re-examine this interdependence, especially as long as non-seismic constraints on $\alpha_{\rm ml}$ are not available.

Concerning the surface effects themselves, we find that with a Gaussian prior on $\alpha_{\rm ml}$, only a few stars in our sample actually require larger corrections. Six stars in our sample do not show strong evidence for any surface effect at all. Compared to the results in Mathur20, this suggests that for many stars taking into account the

radiative losses is already good enough. On the other hand, using only models with $\alpha_{\rm ml} = 1.8$ leads to more significant detections. Irrespective of the prior on $\alpha_{\rm ml}$, we also discovered that the stars for which we do find a highly significant surface effect appear to be located very close to the Sun in the HR diagram (see Fig. 8). A comparison with the stars that were used to derive the traditional surface-effect correction (Kjeldsen et al. 2008) shows that most of these calibrators – including the Sun – also fit the picture. As radiative losses are already taken into account in our models, the modelling of convection and its dependencies on element abundances, opacities and the equation of state remains a leading candidate to explain the cause of the surface effects.

To conclude, although systematic differences between stellar evolutionary codes are still affecting the individual stellar parameters, the systematic analysis of surface effects can already be pursued using more advanced methods than the standard surface correction, such as our Bayesian approach. No matter which surface correction is used, however, the constraints on $\alpha_{\rm ml}$ will potentially affect the results in the absence of lower order modes. The data sets on which this analysis is based have since been superseded by many more quarters of *Kepler* data. Also, many more stars have been observed for which public frequencies are also available (Appourchaux et al. 2012). Strong spectroscopic constraints and access to lower order modes will be necessary to improve our analysis, and to see whether the 'surface effect locus' can be reproduced with a larger sample of stars and better data. Given the large number of subgiants and red giants observed with *Kepler* and *CoRoT*, a similar study for non-main-sequence stars could be very illuminating as well.

ACKNOWLEDGEMENTS

MG, DBG and KM acknowledge funding from the Natural Sciences and Engineering Research Council of Canada. Computational facilities were provided by ACEnet, which is funded by the Canada Foundation for Innovation (CFI), Atlantic Canada Opportunities Agency (ACOA) and the provinces of Newfoundland and Labrador, Nova Scotia and New Brunswick. TK acknowledges financial support from the Austrian Science Fund (FWF P23608).

REFERENCES

Alexander D. R., Ferguson J. W., 1994, ApJ, 437, 879
Appourchaux T. et al., 2012, A&A, 543, A54
Bahcall J. N., Ulrich R. K., 1988, Rev. Modern Phys., 60, 297
Bahcall J. N., Pinsonneault M. H., Wasserburg G. J., 1995, Revi. Modern Phys., 67, 781
Bahcall J. N., Pinsonneault M. H., Basu S., 2001, ApJ, 555, 990
Böhm-Vitense E., 1958, Z. Astrophys., 46, 108
Borucki W. J. et al., 2010, Sci, 327, 977
Brandão I. M. et al., 2011, A&A, 527, A37
Carter J. A. et al., 2012, Sci, 337, 556
Chandrasekhar S., 1957, An Introduction to the Study of Stellar Structure. Dover Press, New York
Chaplin W. J. et al., 2011, Sci, 332, 213
Demarque P., Guenther D. B., Li L. H., Mazumdar A., Straka C. W., 2008, Ap&SS, 316, 31
Eggenberger P., Charbonnel C., Talon S., Meynet G., Maeder A., Carrier F., Bourban G., 2004, A&A, 417, 235
Feroz F., Hobson M. P., Bridges M., 2009, MNRAS, 398, 1601
Grigahcène A., Dupret M.-A., Sousa S. G., Monteiro M. J. P. F. G., Garrido R., Scuflaire R., Gabriel M., 2012, MNRAS, 422, L43
Gruberbauer M., Guenther D. B., 2013, MNRAS, 432, 417
Gruberbauer M., Guenther D. B., Kallinger T., 2012, ApJ, 749, 109 (Paper I)
Guenther D. B., 1994, ApJ, 422, 400
Guenther D. B., Brown K. I. T., 2004, ApJ, 600, 419
Hayashi C., 1961, PASJ, 13, 450
Huber D. et al., 2011, ApJ, 743, 143
Iglesias C. A., Rogers F. J., 1996, ApJ, 464, 943
Jeffreys H., 1961, Theory of Probability, 3rd edn. Oxford Univ. Press, Oxford
Kallinger T. et al., 2010, A&A, 522, A1
Kjeldsen H., Bedding T. R., Christensen-Dalsgaard J., 2008, ApJ, 683, L175
Lane J. H., 1869, Am. J. Sci., 2nd Ser., 50, 57
Mathur S. et al., 2012, ApJ, 749, 152 (Mathur20)
Metcalfe T. S., Creevey O. L., Christensen-Dalsgaard J., 2009, ApJ, 699, 373
Metcalfe T. S. et al., 2010, ApJ, 723, 1583
Metcalfe T. S. et al., 2012, ApJ, 748, L10
Michel E. et al., 2008, Sci, 322, 558
Miglio A. et al., 2013, MNRAS, 429, 423
Palla F., Stahler S. W., 1999, ApJ, 525, 772
Robinson F. J., Demarque P., Li L. H., Sofia S., Kim Y.-C., Chan K. L., Guenther D. B., 2003, MNRAS, 340, 923
Rogers F. J., 1986, ApJ, 310, 723
Rogers F. J., Swenson F. J., Iglesias C. A., 1996, ApJ, 456, 902
White T. R. et al., 2013, MNRAS, 433, 1262

This paper has been typeset from a TEX/LATEX file prepared by the author.